Frontiers of Information Technology & Electronic Engineering
www.jzus.zju.edu.cn; engineering.cae.cn; www.springerlink.com
ISSN 2095-9184 (print); ISSN 2095-9230 (online)
E-mail: jzus@zju.edu.cn

A novel topology with controllable wideband baseband impedance for power amplifiers*

Yao YAO[1], Zhijiang DAI[†‡2], Mingyu LI[2]

[1]*School of Intelligent Technology and Engineering, Chongqing University of Science and Technology, Chongqing 400065, China*

[2]*School of Microelectronics and Communication Engineering, Chongqing University, Chongqing 400065, China*

[†]E-mail: daizj_ok@126.com

Received Feb. 8, 2023; Revision accepted May 17, 2023; Crosschecked Oct. 25, 2023; Published online Dec. 7, 2023

Abstract: This paper presents a novel topology to control the baseband impedance of a power amplifier (PA) to avoid performance deterioration in concurrent dual-band mode. This topology can avoid pure resonance of capacitors and inductors *LC*, which leads to a high impedance at some frequency points. Consequently, it can be applied to transmitters that are excited by broadband signals. In particular, by adjusting the circuit parameters and increasing stages, the impedance of the key frequency bands can be flexibly controlled. A PA is designed to support this design idea. Its saturated output power is around 46.7 dBm, and the drain efficiency is >68.2% (1.8–2.3 GHz). Under concurrent two-tone excitation, the drain efficiency reaches around 40% even under 5.5 dB back-off power with the tone spacing from 10 MHz to 500 MHz. These results demonstrate that the proposed topology is capable of controlling wideband baseband impedance.

Key words: Baseband impedance; Concurrent dual-band; Power amplifier
https://doi.org/10.1631/FITEE.2300074 **CLC number:** TN722

1 Introduction

With the development of mobile communication, the bandwidth of the transmitted signal must be increased to improve the amount of information transmitted per unit time, such as the reported broadband and dual-band power amplifiers (PAs) (Liu et al., 2020; Kilinc et al., 2022; Latha and Rawat, 2022; Li M et al., 2022; Sheikhi and Hemesi, 2022). This requires that PAs can transmit broadband signals, and because the signal's instantaneous bandwidth may exceed 400 MHz, new challenges have emerged in the design of PAs. Efficiency and linearity would be the key indicators (Li C et al., 2019; Feng et al., 2022; Cui et al., 2023). Because of the influence of the transistor's nonlinear capacitance and nonlinear operating state, the baseband signal will be generated under multi-tone/broadband signal excitation. Conversely, the baseband signal will act on the transistor, which influences the memory effect and produces new modulation components.

The effect of baseband impedance was verified by adding different inductors and capacitors in the bias network, and good linear results were obtained by choosing an appropriate bias network in Brinkhoff and Parker (2003) and Brinkhoff et al. (2003). In the dual-band concurrent scenario, Chen et al. (2013) conducted in-depth research on overdrive effects. Nunes et al. (2018) showed that the baseband impedance of the output is the dominant factor in efficiency degradation. Barros et al. (2019)

‡ Corresponding author

* Project supported by the National Natural Science Foundation of China (No. 62001061), the Science and Technology Research Program of Chongqing Municipal Education Commission, China (No. KJQN202201525), the Natural Science Foundation of Chongqing, China (No. CSTB2022NSCQ-MSX0453), and the Research Foundation of Chongqing University of Science and Technology, China (No. CKRC2020029)

ORCID: Zhijiang DAI, https://orcid.org/0000-0003-4914-1464

further showed that both input and output baseband impedances impact the PA performance. As presented in Nunes et al. (2018), efficiency degradation can reach 18%.

Previous studies have shown that the baseband impedance significantly impacts PA performance. The critical point was to avoid resonance in the baseband frequency band, where a high impedance will be presented at the current source plane. The baseband impedance was controlled by carefully designing the bias network in Nunes et al. (2018) and Barros et al. (2019). Although Zhu et al. (2017) proposed an in-package output impedance matching topology, it supports 395 MHz instantaneous bandwidth, and the output matching network needs to be carefully designed to prevent resonance.

When the baseband frequency is close to the operating frequency band, it is difficult to control flexibly, because capacitors need to be added in the power supply network in traditional baseband impedance control methods. However, there is a certain physical distance from the package of the transistor to the position of the filter capacitor, so it is difficult to obtain a low baseband impedance in a wide frequency band. In addition, the direct current (DC) bias capacitors may cause resonance, which results in high impedance at some frequency points. Therefore, in this paper we propose a novel topology to control baseband impedance covering the 10–500 MHz band, which can prevent PA performance deterioration under concurrent dual-band mode.

2 Analysis of the proposed topology

2.1 Analysis of an LC resonant network

It is well known that the expression of two parallel impedances ($Z_A = R_A + \mathrm{j}X_A, Z_B = R_B + \mathrm{j}X_B$) can be written as

$$Z_{AB} = Z_A // Z_B = \frac{(R_A + \mathrm{j}X_A)(R_B + \mathrm{j}X_B)}{R_A + R_B + \mathrm{j}(X_A + X_B)}. \quad (1)$$

If $R_A = 0$ and $R_B = 0$, then $Z_{AB} \to \infty$ when $X_A = -X_B$.

Furthermore, the input impedance function of a pure LC network can be expressed as (Wing, 2008)

$$Zs = K\frac{s^i(s^2+\omega_1^2)(s^2+\omega_3^2)\cdots(s^2+\omega_{2n+1}^2)}{s^j(s^2+\omega_2^2)(s^2+\omega_4^2)\cdots(s^2+\omega_{2n}^2)}, \quad (2)$$

where $i = 0, j = 1$ or $i = 1, j = 0$. K is a constant, and ω_m ($m = 1, 2, ...$) are the poles or zeros of reactance function. There are two conclusions: (1) the reactance function of an LC impedance function has a non-negative slope for all ω; (2) the poles and zeros of an LC impedance (admittance) function alternate on the jω-axis. This means that if the baseband impedance is controlled only through the bias branch with a pure LC network, the LC impedance function will circle around the edge of the Smith chart. In other words, controlling the baseband impedance with a small value in a broad bandwidth would be difficult. If it can be realized, it needs to depend on the parasitic resistance of L or C. Therefore, it is necessary to propose a topology that can accurately control baseband impedance.

2.2 Proposed topology

A topology is proposed for avoiding the resonance mentioned above, as shown in Fig. 1. The baseband impedance control unit (BICU) is connected in parallel with the input/output matching network, and each unit is composed of a microstrip transmission line (TL), a radio frequency (RF) capacitor C_{RF}, a resistor R_{bb}, and a low-frequency capacitor C_{SR}. The primary function of RF capacitor C_{RF} is to short the RF signal and reduce the loss of the fundamental signal in the BICU. The function of C_{SR} is to form series LC resonance with the circuit between points A and C_i, or B and D_j (as marked in Fig. 1) and to reduce the baseband impedance. The R_{bb} function is introduced to avoid pure LC resonance among the BICUs. To control the baseband impedance in a wideband, four BICUs are shunted in the input and output matching networks.

In this way, the impedance of each BICU can be written as

$$Z_{\mathrm{BB},i} = Z_{\mathrm{TL},i}\frac{(R_{\mathrm{eq},i} + 1/(\mathrm{j}\omega C_{\mathrm{bb},i})) + \mathrm{j}Z_{\mathrm{TL},i}\tan(\beta l)}{Z_{\mathrm{TL},i} + \mathrm{j}(R_{\mathrm{eq},i} + 1/(\mathrm{j}\omega C_{\mathrm{bb},i}))\tan(\beta l)}, \quad (3)$$

where $C_{\mathrm{bb},i}$ and $R_{\mathrm{eq},i}$ are the equivalent capacitance and resistance of the i^{th} BICU at point C (D), and the impedance function can be written as

$$Z_{\mathrm{BB,package}} = Z_{\mathrm{BB},1} // Z_{\mathrm{BB},2} // Z_{\mathrm{BB},3} // \cdots. \quad (4)$$

To intuitively describe the circuit characteristics of the proposed topology, the BICU parameters are assigned to observe how the overall equivalent impedance changes. First, several parameters

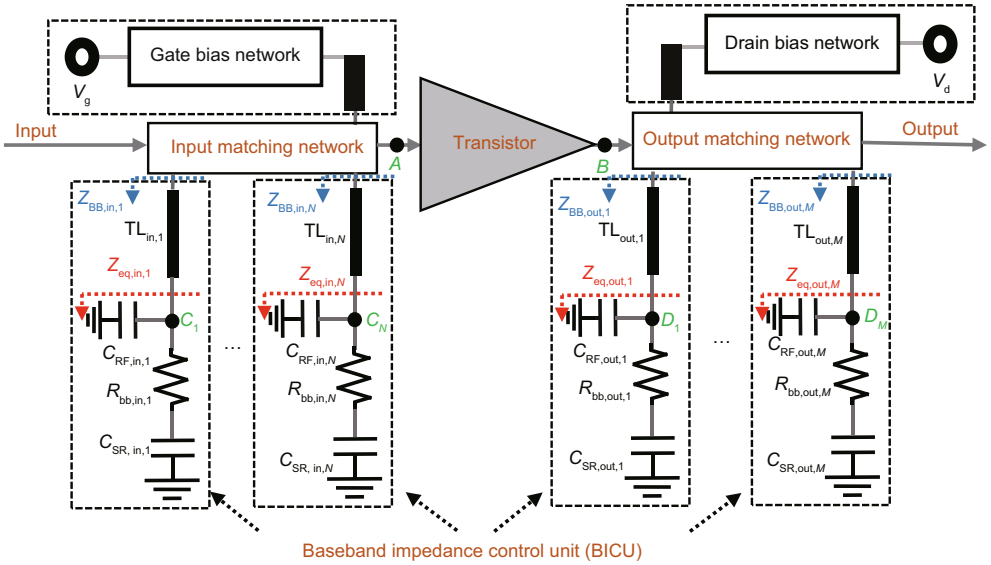

Fig. 1 The proposed topology to control baseband impedance ($Z_{\mathrm{eq,in},i} = 1/(\mathrm{j}\omega C_{\mathrm{bb,in},i}) + R_{\mathrm{eq,in},i}$, $Z_{\mathrm{eq,out},j} = 1/(\mathrm{j}\omega C_{\mathrm{bb,out},j}) + R_{\mathrm{eq,out},j}$)

are determined: the transmission line's characteristic impedance is 77 Ω and the electrical length is 90° at 2.2 GHz. C_{RF} is a 10 pF capacitor of the Murata GRM series. C_{SR} values of the three BICUs are 18, 35, and 70 pF. Then $Z_{\mathrm{BB,package}}$ change could be observed under different values of R_{bb} ($R_{\mathrm{bb}} = \{3, 5, 8, 12\}$ Ω). $Z_{\mathrm{BB},i}$ values of the three BICUs are shown in Fig. 2a, and the impedance curves of the three cases are shown in Fig. 2b. It can be seen from Fig. 2 that the selection of R_{bb} is neither the higher the better, nor the smaller the better. R_{bb} needs to be flexibly selected according to the BICU parameters and the number of parallel circuits; otherwise, the high impedance of Z_{BB} or a local resonance point (reactance value becomes larger) would occur.

In general, multiple parallel BICUs are used simultaneously to control the baseband impedance with a small value in a wide frequency band, and each selected BICU is used to manage the baseband impedance at different frequency points (f_1, f_2, ...). An appropriate $C_{\mathrm{SR},i}$ is used to form a resonance with corresponding TL_i at f_i, so the impedance value of $Z_{\mathrm{BB},i}$ at f_i is small. Due to the existence of R_{bb}, multiple parallel BICUs can achieve a small baseband impedance in a wideband by using Eq. (4). Then if we design BICUs carefully, the baseband impedance can be adequately controlled in a wideband, and high impedance resonance state can be avoided by using BICUs.

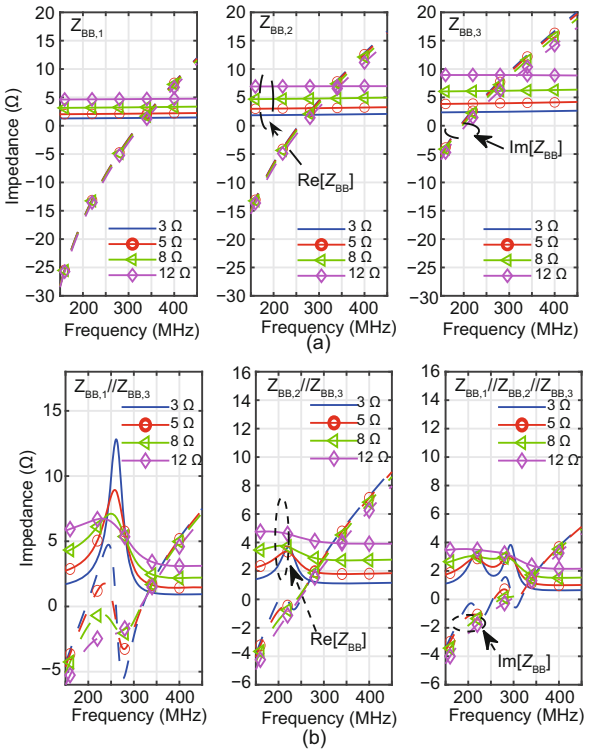

Fig. 2 $Z_{\mathrm{BB},i}$ under different $C_{\mathrm{SR}} = \{18, 35, 70\}$ pF (a) and three cases of Z_{BB} with different baseband impedance control units (BICUs) (b). The solid and dotted lines represent the real and imaginary parts of $Z_{\mathrm{BB},i}$ or Z_{BB}, respectively

Z_{BB} of a BICU changing along with R_{bb} and C_{SR} is given in Fig. 3. It can be seen that the

imaginary part of $Z_{\rm BB}$ depends mainly on $C_{\rm SR}$. The real part of $Z_{\rm BB}$ will change greatly with $R_{\rm bb}$ and $C_{\rm SR}$. Therefore, in the design, we can first define the resonant frequency point through $C_{\rm SR}$, and then adjust the impedance $Z_{\rm BB}$ by changing $R_{\rm bb}$.

The parameters of the BICUs can be determined using the following procedures: (1) First, choose the size of TL (length and width) according to the working frequency band, and select RF capacitor $C_{\rm RF}$ according to the operating frequency band. (2) Determine the resonant frequency points of the BICUs and the number of BICUs, and calculate $C_{\rm SR}$. Let each resonant frequency point be dispersed in the target frequency band. (3) Adjust $R_{\rm bb}$ to make $Z_{\rm BB}$ as small as possible on the package plane and meet the target requirements, such as $|Z_{\rm BB,package}| < 5\ \Omega$.

2.3 Design example

A PA working in the 1.8–2.3 GHz band is designed as an example to explain how to control baseband impedance. The output matching network is given in Fig. 4 with four BICUs. Four BICUs are as close to the package of transistors as possible to achieve a small baseband impedance in the 0–500 MHz band. Accordingly, the impedance at the low-frequency band is provided in Fig. 5a when $R_{\rm bb} = 0.1\ \Omega$ and $R_{\rm bb} = 6\ \Omega$. By comparing these two cases, it can be found that when the impedance $R_{\rm bb}$ is close to 0, the resonance phenomenon will appear in the circuit, leading to impedance spikes at some frequency points, i.e., {55, 130, 235, 380} MHz, which will worsen the PA performance in the concurrent mode. The fundamental and harmonic impedances are plotted in Fig. 5b. It

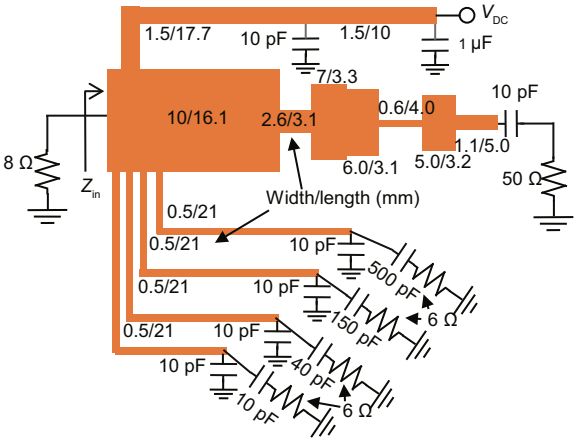

Fig. 4 Output matching network with four baseband impedance control units

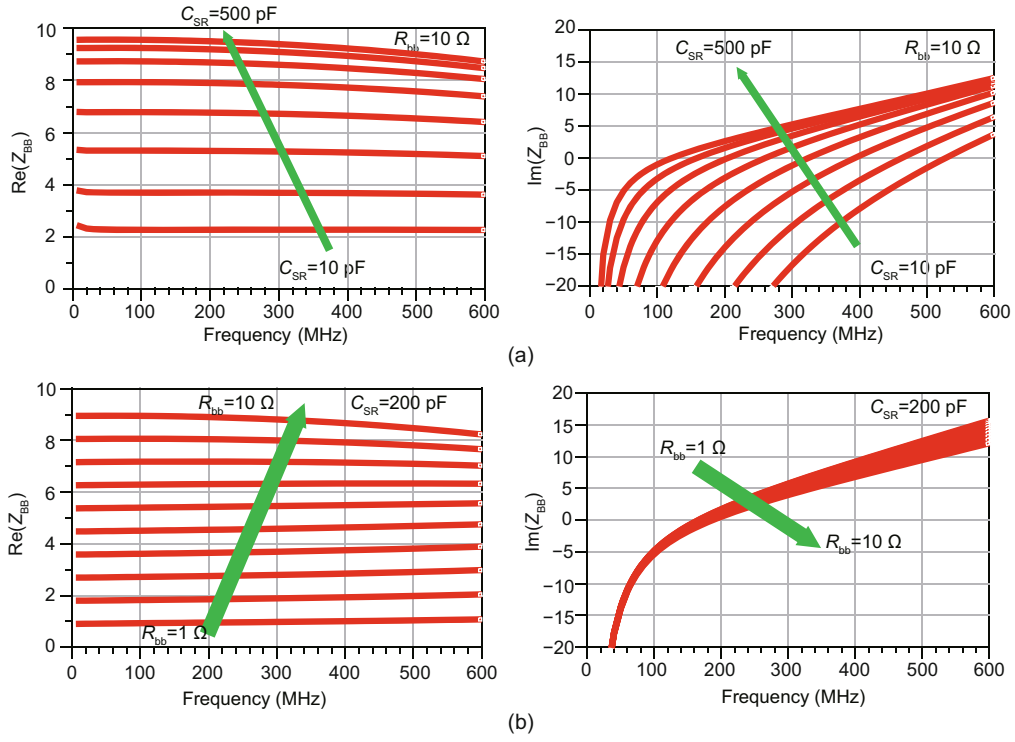

Fig. 3 Impedance of a baseband impedance control unit: (a) $Z_{\rm BB}$ vs. $C_{\rm SR}$; (b) $Z_{\rm BB}$ vs. $R_{\rm bb}$

could be found that BICUs have little influence on harmonic impedance.

On the other hand, to evaluate the impact of the BICU on the fundamental impedance and loss of the matching network, the fundamental impedance and S_{21} values are shown in Fig. 6 (the circuit parameters are the same as those in Fig. 4). The simulation results show that it has little effect on the fundamental impedance, while the maximum loss in the 1.5–2.6 GHz band is <0.05 dB.

This shows that by using this topology, the low-frequency baseband impedance can be adjusted with little effect on fundamental frequency impedance. In other words, it can achieve good PA performance in the concurrent mode without affecting its performance in the narrowband mode.

Under two-tone excitation, the efficiency and IMD3 (the difference between the output power and three-order intermodulation product in dBc) with different numbers of BICUs are shown in Fig. 7 when the output power of each tone is 35 or 38 dBm. Observing Figs. 2b and 5a, we can see that the impedance within the 500 MHz frequency band is relatively small at three and four BICUs (their impedance is <5 Ω). From the simulation results, it can also be seen that their performance is similar. In actual experiments, to flexibly adjust the parameters of the circuit, we choose a topology structure of four BICUs.

It is worth noting that when the number of BICUs exceeds 3, the parasitic reactance from the transistor packaging plane to the current source plane significantly impacts the baseband impedance. However, due to the commercial transistor limitations, the parasitic network part cannot be changed. This leads to inability to design baseband impedance.

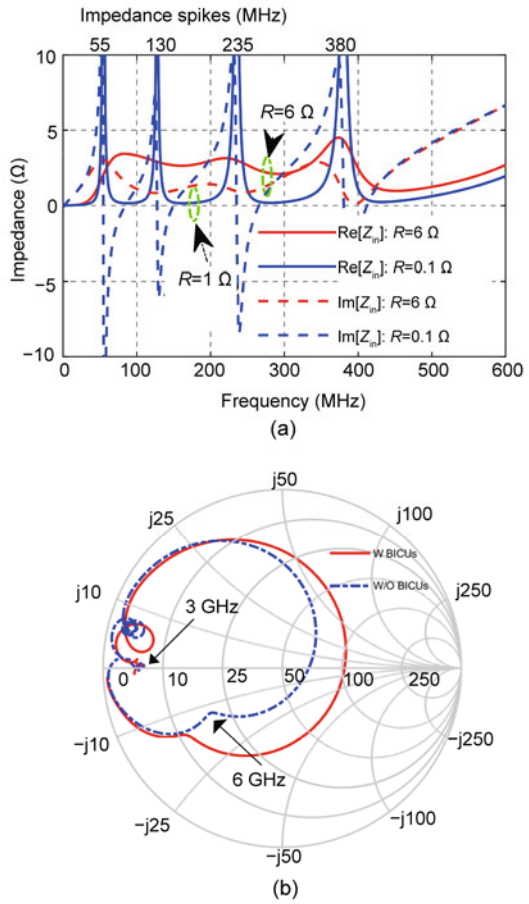

Fig. 5 Output matching: (a) impedance with different R_{bb}; (b) S_{11} with/without baseband impedance control units in 1.5 to 7.0 GHz (w: with; w/o: without; BICUs: baseband impedance control units)

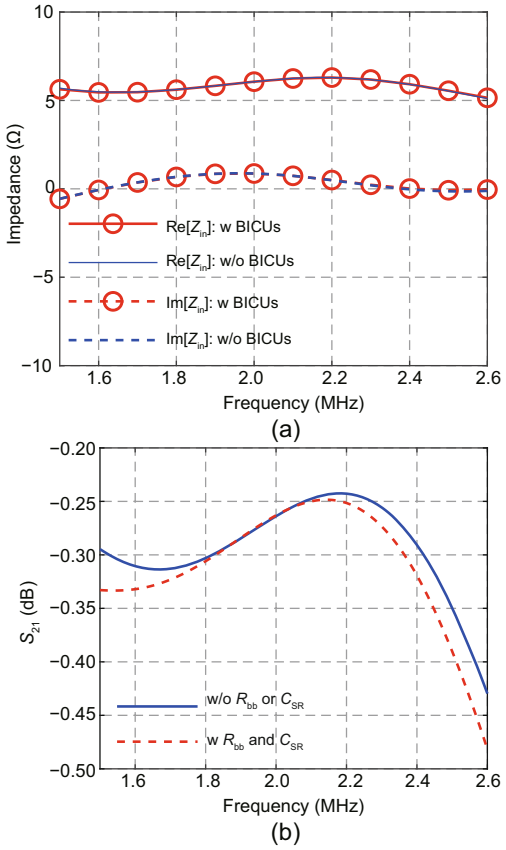

Fig. 6 Output matching network simulation: (a) input impedance with/without C_{RF} and R_{bb}; (b) S_{21} with/without C_{RF} and R_{bb} (w: with; w/o: without; BICUs: baseband impedance control units)

3 Measurement results

The adopted printed circuit board (PCB) is Rogers 4350B with a thickness of 0.508 m (ε_r = 3.66), and a Wolfspeed CGH40045 GaN transistor is used to verify our proposed approach. Fig. 8 is a photograph of the implemented PA. BICUs are added in the input and output matching networks.

First, under the excitation of a single-tone continuous wave, the saturation output power and drain efficiency are presented in Fig. 9. The measured saturated output power and efficiency range from 46.3 to 47.1 dBm and 68.2% to 71.6% within the 1.8–2.3 GHz band, respectively, where gain compression is about 3 dB. Because the efficiency curve of this band is relatively flat (about ±1.7%), this band is selected to evaluate the performance of PA under two-tone excitation and increasing spacing. The simulated and measured results show that the PA efficiency is higher without BICUs than that with BICUs in continuous single-tone mode.

Furthermore, with the excitation of a two-tone (F_1 and F_2) continuous wave, the output powers of the two frequency bands are equal by independently adjusting the input signal power of the two frequency points. The test block diagram is given in Fig. 10. With the increasing tone spacing from 10 to 500 MHz (i.e., spacing=$F_2 - F_1$), simulated and measured efficiency and IMD3 at two output power levels (35 and 38 dBm) are shown in Figs. 11 and 12 respectively, where we determine whether to connect BICUs by cutting or not cutting the transmission lines in BICUs. It can be observed in Figs. 11 and 12 that using BICUs can improve efficiency, at least, when the frequency is >180 MHz. The measured efficiency is about 28.5% when the output power per

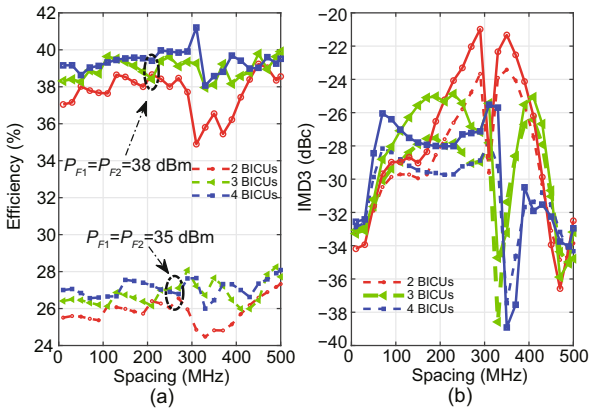

Fig. 7 Simulated efficiency (a) and IMD3 (b) with different numbers of baseband impedance control units (BICUs) and output power

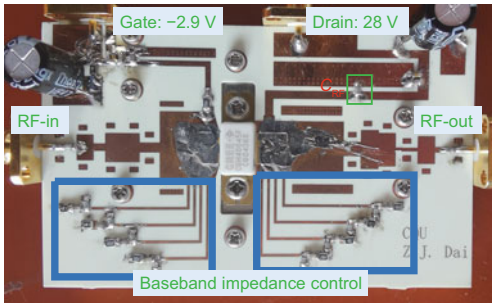

Fig. 8 Fabricated printed circuit board

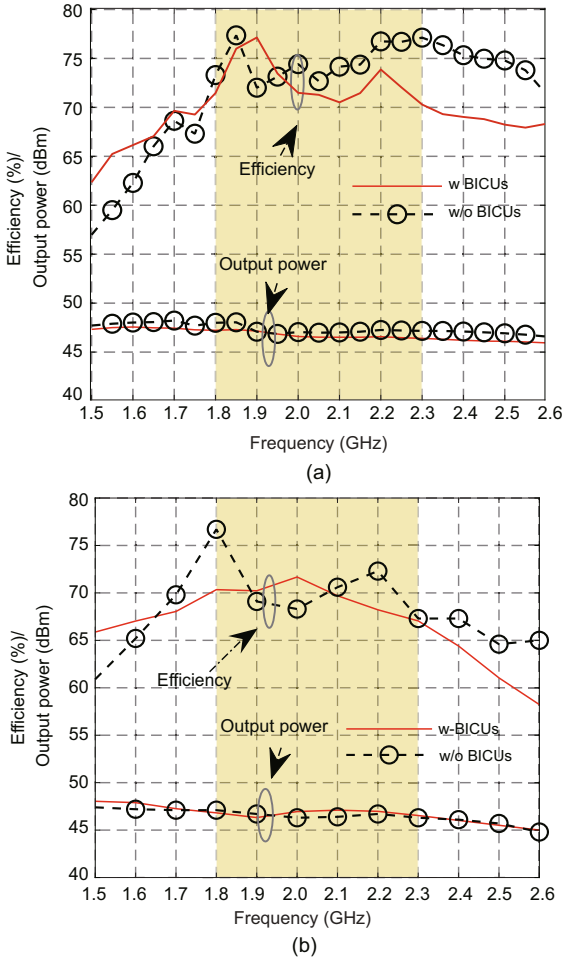

Fig. 9 Efficiency and output power vs. frequency with/without baseband impedance control units (BICUs): (a) simulation; (b) measurement

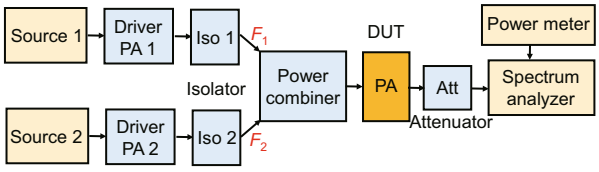

Fig. 10 Test block diagram under two-tone excitation

tone is 35 dBm (about 8.5 dB power back-off). The measured efficiency is about 40% when the output power per tone is 38 dBm (about 5.5 dB power back-off). When the output power of each tone is 35 and 38 dBm, IMD3 is about −34 and −27 dBc in the 10–300 MHz range and −22 and −22 dBc in the 300–500 MHz range, respectively. Compared with test and simulation results, efficiency values are compatible. The simulation results and test IMD3 are not consistent within the 300–500 MHz band. The main reasons are: (1) the parasitic parameters of the lumped elements used in the circuit have a significant influence in the 300–500 MHz band; (2) IMD3 is related to the impedance at the frequency of F_1+F_2, which may have a large deviation from the simulation results.

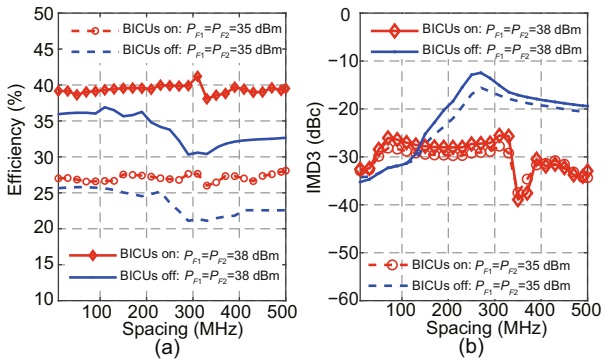

Fig. 11 Simulated efficiency (a) and IMD3 (b) under concurrent two-tone excitation (F_1=1.8 GHz, F_2 = F_1+spacing)

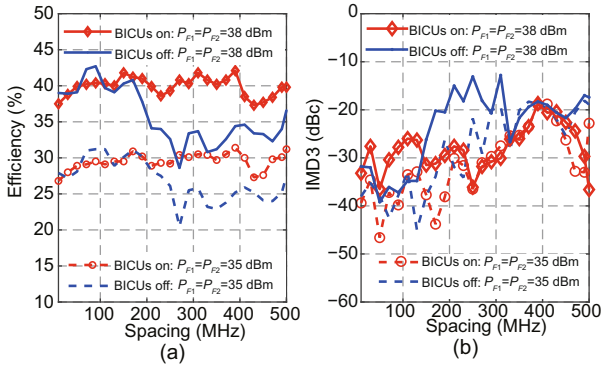

Fig. 12 Measured efficiency (a) and IMD3 (b) under concurrent two-tone excitation (F_1=1.8 GHz, F_2 = F_1+spacing)

Comparison is given in Table 1. It could be noted that the proposed topology is competent for wideband baseband impedance control.

4 Conclusions

In this paper, a novel baseband impedance control network topology is proposed, and a power amplifier design example is presented to explain the application of the topology. The experimental results show that the baseband impedance can be controlled up to 500 MHz with low impedance, and that there is no resonance generation when four parallel BICUs are used. In addition, the proposed topology can help avoid PA efficiency deterioration with an increase in the tone spacing. This topology offers an opportunity to control more complex baseband impedance with more BICUs, such as the application of tri-band concurrent mode.

Contributors

Yao YAO and Zhijiang DAI designed the research. Yao YAO drafted the paper. Mingyu LI helped organize the paper. Zhijiang DAI revised and finalized the paper.

Compliance with ethics guidelines

Yao YAO, Zhijiang DAI, and Mingyu LI declare that they have no conflict of interest.

Data availability

The data that support the findings of this study are available from the corresponding author upon reasonable request.

References

Barros DR, Nunes LC, Cabral PM, et al., 2019. Impact of the input baseband terminations on the efficiency of wideband power amplifiers under concurrent band operation. *IEEE Trans Microw Theory Techn*, 67(12):5127-5138. https://doi.org/10.1109/TMTT.2019.2951147

Brinkhoff J, Parker AE, 2003. Effect of baseband impedance on FET intermodulation. *IEEE Trans Microw Theory*

Table 1 Comparison with reported power amplifiers under two-tone excitation

Reference	Baseband bandwidth (MHz)	Center frequency (GHz)	IMD3 (dBc)	Output power (dBm)	DE (%)
Chen et al., 2013	10–15	1.9/2.7	–	36.5	38*
Nunes et al., 2018	10–400	2.0	–	44.5*	43*
Barros et al., 2019	50–400	2.55	−30–−22	39	42*
This work	10–500	2.0	−27–−22	41	40

* Estimation results. DE: drain efficiency

Techn, 51(3):1045-1051. https://doi.org/10.1109/TMTT.2003.808704

Brinkhoff J, Parker AE, Leung M, 2003. Baseband impedance and linearization of FET circuits. *IEEE Trans Microw Theory Techn*, 51(12):2523-2530. https://doi.org/10.1109/TMTT.2003.819208

Chen XF, Chen WH, Ghannouchi FM, et al., 2013. Enhanced analysis and design method of concurrent dual-band power amplifiers with intermodulation impedance tuning. *IEEE Trans Microw Theory Techn*, 61(12):4544-4558. https://doi.org/10.1109/TMTT.2013.2282283

Cui J, Li PP, Sheng WX, 2023. High linearity U-band power amplifier design: a novel intermodulation point analysis method. *Front Inform Technol Electron Eng*, 24(1):176-186. https://doi.org/10.1631/FITEE.2200082

Feng WJ, Wu WB, Zhou XY, et al., 2022. Broadband high-efficiency quasi-class-J power amplifier based on nonlinear output capacitance effect. *IEEE Trans Circ Syst II Expr Briefs*, 69(4):2091-2095. https://doi.org/10.1109/TCSII.2022.3141423

Kilinc S, Yarman BS, Ozoguz S, 2022. Broadband power amplifier design via fictitious matching. *IEEE Trans Circ Syst II Expr Briefs*, 69(12):4844-4848. https://doi.org/10.1109/TCSII.2022.3207423

Latha YMA, Rawat K, 2022. Design of ultra-wideband power amplifier based on extended resistive continuous class B/J mode. *IEEE Trans Circ Syst II Expr Briefs*, 69(2):419-423. https://doi.org/10.1109/TCSII.2021.3095379

Li C, You F, He SB, et al., 2019. High-efficiency power amplifier employing minimum-power harmonic active load modulator. *IEEE Trans Circ Syst II Expr Briefs*, 66(8):1371-1375. https://doi.org/10.1109/TCSII.2018.2883685

Li M, Li ZQ, Zheng Q, et al., 2022. A 17–26.5 GHz 42.5 dBm broadband and highly efficient gallium nitride power amplifier design. *Front Inform Technol Electron Eng*, 23(2):346-350. https://doi.org/10.1631/FITEE.2000513

Liu X, Lv GS, Wang DH, et al., 2020. Energy-efficient power amplifiers and linearization techniques for massive MIMO transmitters: a review. *Front Inform Technol Electron Eng*, 21(1):72-96. https://doi.org/10.1631/FITEE.1900467

Nunes LC, Barros DR, Cabral PM, et al., 2018. Efficiency degradation analysis in wideband power amplifiers. *IEEE Trans Microw Theory Techn*, 66(12):5640-5651. https://doi.org/10.1109/TMTT.2018.2871199

Sheikhi A, Hemesi H, 2022. Analysis and design of the novel class-F/E power amplifier with series output filter. *IEEE Trans Circ Syst II Expr Briefs*, 69(3):779-783. https://doi.org/10.1109/TCSII.2021.3112974

Wing O, 2008. Classical Circuit Theory. Springer, New York, USA.

Zhu N, McLaren R, Holmes DG, et al., 2017. An integrated RF match and baseband termination supporting 395 MHz instantaneous bandwidth for high power amplifier applications. Proc IEEE MTT-S Int Microwave Symp, p.1114-1117. https://doi.org/10.1109/MWSYM.2017.8058791